MODELLING OF PRESSURE DISTRIBUTIONS OVER FUEL-STRINGS FOR FUEL IRRADIATION EXPERIMENTS IN THE NRU REACTOR

E. Nihan. Onder and Laurence K.H. Leung

Atomic Energy of Canada Limited, Thermalhydraulics Branch,
Chalk River Laboratories, Chalk River, ON K0J 1J0 Canada

ABSTRACT

A pressure-drop model has been developed for the U-1 and U-2 loops of the NRU reactor. It provides local pressure distributions between instrument locations at the inlet and outlet of each loop. Piping components and fuel-string assemblies are modeled for single-phase and two-phase flows. The overall pressure drop comprises frictional and form losses, as well as changes due to acceleration and gravity. Detailed pressure profiles have been established along the U-1 and U-2 loops at two powers. The pressure loss over the fuel string is typically larger than losses over the inlet, connecting, and outlet piping components. A linear pressure profile has been observed over the fuel string at low power, indicating single-phase flow in the channel. The pressure profile becomes non-linear at high power, signifying the presence of two-phase flow at the downstream end. Different combinations of fuel type in the string appear to have little impact on the pressure profile. This is mainly due to the similarity of pressure-drop characteristics of the fuel types used in fuel irradiation experiments.

1. INTRODUCTION

The National Research Universal (NRU) reactor is a heavy-water cooled and moderated research reactor, with on-line refueling capability. It is mainly used to produce neutrons for radioisotope production, fuel testing, material testing, and fundamental research. The U-1 and U-2 test loops of the NRU reactor are designed for fuel and material irradiation experiments at high pressures and high temperatures with light water as a coolant. Figure 1 shows schematically the channel configurations in the U-1 and U-2 loops. Axial pressure distributions along these loops are required for analyses of critical channel power and hydride formation. Thus, it is the objective of this study to derive a pressure-drop model to accurately predict the axial pressure distribution along the channels of U-1 and U-2 loops.

The pressure-drop model covers all sections between the instrument locations for pressure and fluid-temperature measurements at the inlet and outlet ends of each loop. Simple pipes, annuli, and piping components are included in most sections. The main components of each fuel-string section are six fuel bundles and upper and lower flux suppressors. Several bundle types are employed in fuel-irradiation experiments: CANDU®[1] 37-element bundles, CANFLEX®[2] bundles, and material-test bundles.

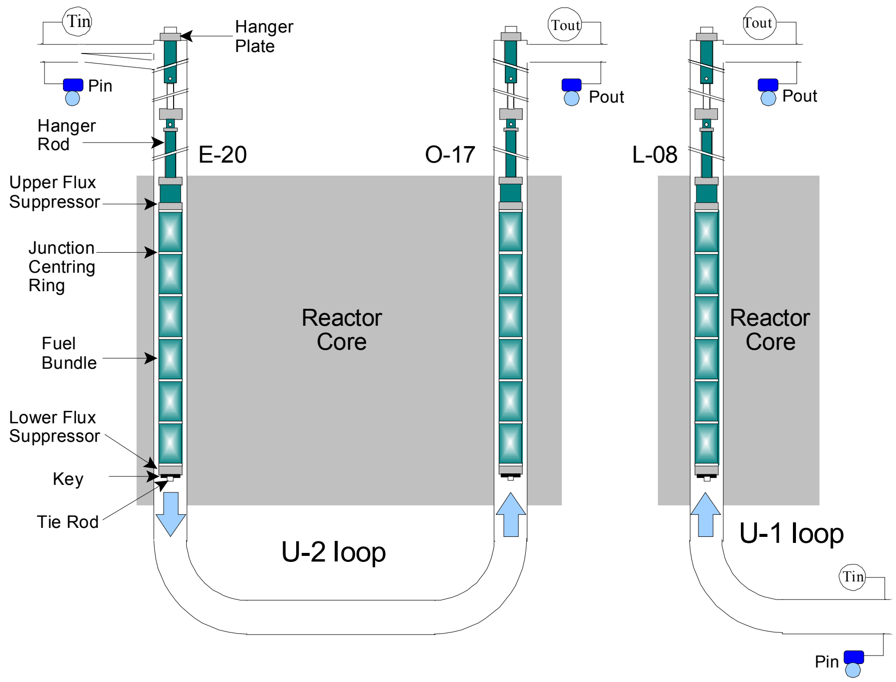

Figure 1 Schematic Diagram of the Channel Configuration in U-1 and U-2 Loops

1.1. U-1 Loop

The U-1 loop consists of a single channel (L-08) for fuel irradiation. Flow is brought in from the bottom of the channel, circulates upward through the fuel string, and discharges from the channel assembly through a branch. Instruments are placed at the inlet pipe and outlet branch of the channel assembly to measure pressures and fluid temperatures. The fuel string is hung from the top of the channel assembly, with bundles located in the high neutron-flux region of the reactor core.

1.2. U-2 Loop

The U-2 loop consists of two channels (E-20 and O-17) for fuel irradiation. Flow is brought in from a branch (split into two smaller branches) at the top of Channel E-20, circulates downward through the upstream fuel string, passes through a series of connecting pipes and elbows at the bottom of the reactor, circulates upward through the downstream fuel string in Channel O-17, and discharges from the O-17 channel assembly through a branch. Instruments are installed at the inlet branch of Channel E-20 and outlet

[1] CANDU® (CANada Deuterium Uranium) is a registered trademark of Atomic Energy of Canada Limited (AECL).
[2] CANFLEX® (CANDU FLEXible) is a registered trademark of AECL and Korea Atomic Energy Research Institute (KAERI).

branch of Channel O-17 to measure pressures and fluid temperatures. Two fuel strings are irradiated in the loop. Each string is hung from the top of the channel assembly, with bundles located in the high neutron-flux region of the reactor core.

2. PRESSURE-DROP MODEL

The pressure-drop model covers all sections, including the inlet and outlet instrument locations, and the fuel string region. Sub-models for pressure-drop calculations over the inlet-flow and outlet-flow regions (as well as the connecting-pipe region in the U-2 loop) are the same for both the U-1 and U-2 loops. Those over the fuel-string region depend on the bundle configuration, and hence are based on bundle-specific correlations.

2.1. Modeling of Pressure Drops over Regions Outside the Fuel String

Pressure drops over regions outside the fuel string are modeled for the following components:

- straight pipes,
- annuli,
- equivalent pipes (to model fixtures, such as the fuel stop, upper flux suppressor, and lower flux suppressor, through flow area and hydraulic-equivalent diameter),
- elbows (45°, 60°, 75° and 90°),
- sudden expansions,
- sudden contractions,
- converging wyes (to model the connecting point between the horizontal pipe at the inlet-flow branch and the vertical channel in Channel E-20), and
- diverging wyes (to model the connecting point between the vertical channel in either Channel O-17 or Channel L-08 and the horizontal pipe at the outlet-flow branch).

In general, the overall pressure drop over regions outside the fuel string (ΔP_{OFS}) is calculated from

$$\Delta P_{OFS} = \Delta P_f + \Delta P_a + \Delta P_g + \Delta P_{form} \tag{1}$$

2.1.1. Frictional-Losses

The single-phase frictional loss is calculated using

$$\Delta P_{f,sp} = \frac{f_{tube}\, L}{D_{hy}} \frac{G^2}{2\rho_b} \tag{1}$$

The friction factor for pipe flow, f_{tube}, is calculated using an explicit form of the Colebrook-White equation [2]

$$f_{tube} = 4\left(3.48 - 1.7372\ln\left(\frac{2\,\varepsilon}{D_{hy}} - \frac{16.2426}{\mathrm{Re}}\ln\left(\frac{(2\varepsilon / D_{hy})^{1.1098}}{6.0983} + \left(\frac{7.149}{\mathrm{Re}}\right)^{0.8981}\right)\right)\right)^{-2} \tag{2}$$

where the roughness height , ε, is assumed to be 10 μm for all surfaces.

The two-phase frictional pressure loss is calculated using

$$\Delta P_{f,\,tp} = \phi^2_{LO,\,f}\ \Delta P_{f,\,sp} \tag{3}$$

The two-phase multiplier for frictional loss $\phi^2_{LO\ ,\ f}$ is calculated from the following, assuming homogeneous flow

$$\phi^2_{LO,\,f} = \left(1 + x\left(\frac{\rho_l}{\rho_v} - 1\right)\right)\left(1 + x\left(\frac{\mu_l}{\mu_v} - 1\right)\right)^{-0.25} \tag{4}$$

The vapour-mass quality is defined as

$$\begin{aligned} x &= 0 && for\ x_{th} \le 0, \\ &= x_{th} && for\ 0 < x_{th} < 1, \\ &= 1 && for\ x_{th} \ge 1. \end{aligned} \tag{5}$$

where the thermodynamic quality, x_{th}, established through a heat balance.

2.1.2. Pressure Drop due to Acceleration

The pressure drop due to acceleration is a measure of momentum changes over a control volume. It is expressed for single-phase flow as

$$\Delta P_{a,\,sp} = \Delta(G^2 v_b) \tag{6}$$

The two-phase pressure drop due to acceleration is calculated assuming homogeneous flow. It is expressed as

$$\Delta P_{a,\,tp} = \Delta\left(G^2\left(\frac{x}{\rho_v} + \frac{(1-x)}{\rho_l}\right)\right) \tag{7}$$

2.1.3. Pressure Drop due to Gravity

The pressure drop due to gravity is a measure of the change in potential energy of the fluid due to change in elevation. It is expressed for single-phase flow as

$$\Delta P_{g,\,sp} = \rho_b\, g\, \Delta z \tag{8}$$

The two-phase pressure drop due to gravity is calculated assuming homogeneous flow

$$\Delta P_{g,\,tp} = (x\,\rho_v + (1-x)\,\rho_l)\, g\, \Delta z \tag{9}$$

2.1.4. Form Losses

Pressure drops over elbows, sudden contractions, sudden expansions, converging wyes, and diverging wyes are considered as form losses (frictional losses are relatively small over these components). In general, the form loss is calculated for single-phase flow using

$$\Delta P_{form,\,sp} = K_{form} \frac{G^2}{2\rho_b} \tag{10}$$

where the form loss coefficient, K_{form}, over the components is established from Idelchik [3].

The two-phase pressure drop due to form loss is calculated using

$$\Delta P_{form,\,tp} = \phi^2_{LO,\,form}\ \Delta P_{form,\,sp} \tag{11}$$

where the two-phase multiplier for form loss, $\phi^2_{LO,\,form}$, is calculated from the following, assuming homogeneous flow

$$\phi^2_{LO,\,form} = \left(1 + x\left(\frac{\rho_l}{\rho_v} - 1\right)\right) \tag{12}$$

2.2. Pressure Drop over the Fuel-String Region

The fuel-string region comprises mainly six fuel bundles for irradiation. The total pressure drop consists of frictional losses, form losses due to appendages and junctions, contraction and expansion losses at the entrance and outlet regions of the fuel string, and pressure drop due to momentum and gravity changes. The sudden-contraction loss is due to flow-area change from either the upper flux suppressor or the lower flux suppressor to the fuel string, while the sudden-expansion loss is due to flow-area change from the fuel string to either the upper flux suppressor or the lower flux suppressor. A junction-centering ring is installed between two bundles. It has a small flow obstruction area and hence is not modeled. The overall pressure drop over the fuel string is expressed as

$$\Delta P_{fuel\ string} = \Delta P_{cont} + \Delta P_{fuel} + \Delta P_{\exp} + \Delta P_a + \Delta P_g \tag{13}$$

Modeling of pressure drop for each component covers both single-phase and two-phase flows, even though components at the inlet end of the fuel string are mainly exposed to single-phase flow. Heating of the coolant is considered only in the fuel-string region, assuming negligible heat losses.

2.2.1. Pressure Drop over the Fuel Bundle

The pressure drop over a string of CANDU bundles consists of a skin-friction component and local form loss components at the junction (primarily caused by the end-plate, rod misalignment and rod discontinuity), spacer plane (due to both spacers and bearing pads), button plane (CANFLEX bundle only), and bearing-pad plane. It is expressed as

$$\Delta P_{fuel} = \Delta P_f + \sum_{i=1}^{n} \Delta P_j + \sum_{i=1}^{m} \Delta P_s + \sum_{i=1}^{j} \Delta P_{bp} + \sum_{i=1}^{k} \Delta P_{but} \tag{14}$$

Combining the friction and local-loss components into a bundle loss coefficient, the single-phase pressure drop over a CANDU bundle is obtained as

$$\Delta P_{fuel,\,sp} = K_{bundle} \frac{G^2}{2\rho_b} = \left(\frac{f_{bundle} L_{bundle}}{D_{hy}} + K_{total} \right) \frac{G^2}{2\rho_b} \tag{15}$$

The bundle friction factor, f_{bundle}, and loss coefficients, K_{bundle} and K_{total}, are generally determined from single-phase pressure drop measurements obtained with production bundles. Single phase experiments were performed for 37-element and CANFLEX bundles at Sheridan Park Engineering Laboratories (SPEL), Korea Atomic Energy Research Institute (KAERI), and Chalk River Laboratories (CRL).

Introducing the same methodology used in the NUCIRC code [1], the bundle friction factor is expressed as

$$f_{bundle} = f_{cor} f_{CW} (1 - \lambda_{cc} C) \tag{16}$$

The reducing factor for the channel creep effect ,λ_{cc} , was derived based on experimental data generated at CRL.

The bundle correction factor depends on the geometry and is expressed as

$$f_{cor} = a - b \,\mathrm{Re} \tag{17}$$

where ”a” and “b” are coefficients derived from experimental pressure-drop data obtained with various bundle types.

The percentage of diametral creep, C, at the location of interest is determined using the local pressure-tube inside diameter for the corresponding channel. It is defined as

$$C = Max\left(0.,\ \frac{D_{P/T} - D_{ref}}{D_{ref}} \right) \tag{18}$$

The total form-loss coefficient is defined as

$$K_{total} = (K_{j,\,mpm} + K_{app})_{uncrept}\ (1 - \lambda_K C) \tag{19}$$

The creep-effect reducing factor, λ_K , and the form-loss coefficients, $K_{j,mpm}$ and K_{app}, were derived based on experimental data generated at CRL.

The two-phase pressure drop for the bundle is calculated with

$$\Delta P_{fuel,\,tp} = \phi^2_{LO,\,fuel}\, \Delta P_{fuel,\,sp} \tag{20}$$

Several experiments were carried out at CRL to derive the two-phase multipliers, $\phi^2_{LO,\,fuel}$, for various bundles, misalignment angle, channel creeps and flow conditions. As a result, a modification factor to the homogeneous two-phase multiplier was introduced.

2.2.2. Pressure Drop due to Acceleration

Calculations for the pressure drop due to acceleration have been described in Section 2.1.2. The single-phase pressure drop due to acceleration is presented in Equation (6). To be consistent with the approach employed in safety analyses, the two-phase pressure drop due to acceleration is calculated with the separated-flow model for bundles. It is expressed as

$$\Delta P_{a,tp} = \Delta\left(G^2 \left(\frac{x_a^2}{\alpha\,\rho_v} + \frac{(1-x_a)^2}{(1-\alpha)\,\rho_l} \right) \right) \tag{21}$$

The void fraction, α, is calculated with the Massena correlation [4], which is expressed as

$$\alpha = \frac{(0.833 + 0.167 x_a) x_a v_v}{(1-x_a) v_l + x_a v_v} \quad \textit{for } 0 < \alpha < 1.0 \tag{22}$$

2.2.3. Pressure Drop due to Gravity

Calculations for the pressure drop due to gravity have been described in Section 2.1.3. The single-phase pressure drop due to gravity is presented in Equation (8). To be consistent with the separate-flow approach employed in safety analyses for bundles, the two-phase pressure drop due to gravity is calculated with

$$\Delta P_{g,tp} = (\alpha\,\rho_g + (1-\alpha)\,\rho_f)\, g\, \Delta z \tag{23}$$

3. PRESSURE PROFILES ALONG THE U-1 AND U-2 LOOPS

Calculated pressure profiles using the pressure-drop model are illustrated in this section for the U-1 and U-2 loops. The pressure-drop model establishes local pressures at various nodes along the loop. Each node corresponds to a piping component (i.e., elbows, sudden contraction, sudden expansion, etc.) and the distance between nodes represents either a pipe (or equivalent) or an annulus in the inlet-flow, outlet-flow and connecting-pipe (only for the U-2 loop) regions. The fuel-string region has been subdivided into twenty-four nodes (i.e., four nodes per bundle).

3.1. Pressure Profiles in the U-1 Loop

Fuel irradiation experiments cover a wide range of inlet fluid temperatures and fuel-string powers in the U-1 loop. A fuel string consisting of six 37-element bundles is used to illustrate the calculation of the axial pressure profile. The flow conditions covered in the calculation are typical and correspond to the time-average value of pressure at 9.66 MPa, the nominal value of mass flow rate at 16.5 $kg.s^{-1}$, and the time-average value of the inlet-fluid temperature at 275°C. Two fuel string powers are applied: one at 2158 kW and the other at 5197 kW.

The pressure-drop model is applied to provide axial pressure profiles in the U-1 loop at the two powers of interest. Figure 2 shows calculated pressure profiles over the inlet branch at the bottom of Channel L08, the fuel assembly, and the outlet branch at the top of Channel L08. The origin for the calculation is assumed at the center of the elbow at the bottom of the channel (see Figure 1). Negative axial distances shown in Figure 2 refer simply to locations upstream of the origin. The overall pressure loss, between instrument locations at inlet and outlet ends, is predicted to be 269 kPa at the low power and 403 kPa at the high power.

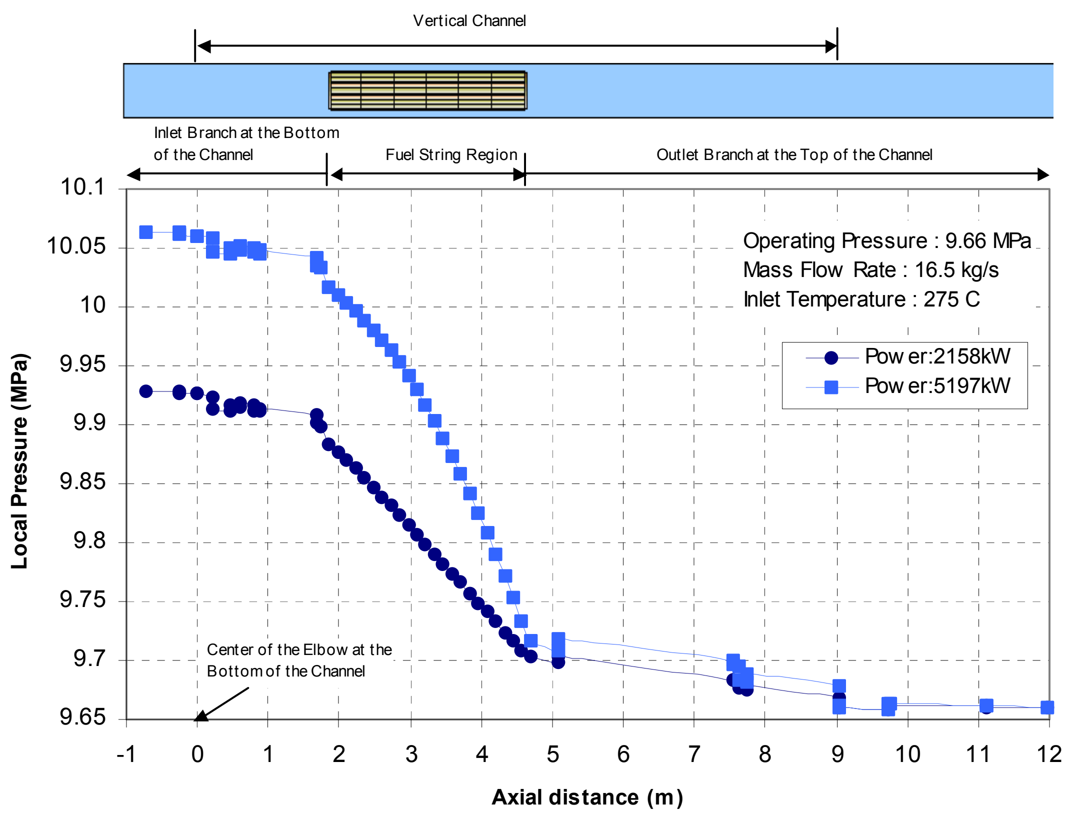

Figure 2 Pressure Profiles along the U-1 Loop.

A sharp drop in pressure at the node represents a sudden contraction, while a pressure rise at the node corresponds to a sudden expansion. In most cases, the flow-area variation in the loop is gradual and smooth. The assumption of sudden variation (i.e., either a contraction or an expansion) results in overpredictions of the pressure loss. Table 1 lists the calculated pressure drop at each region of the U-1 loop.

Table 1 Pressure Drops over Various Regions of the U-1 Loop

	Pressure Drop (kPa)			
	Inlet	Fuel String	Outlet	Overall
Power = 2158 kW	30	195	44	269
Power = 5197 kW	30	317	56	403

The pressure loss over the inlet branch is about 30 kPa at both powers. It is mainly due to components at the bottom of the channel, including expansions, the fuel stop, and the lower flux suppressor. The same pressure drop is predicted because this region consists mainly of single-phase flow at both powers. A sharp pressure drop is predicted over the fuel-string section due to the reduction in flow area, increase in surface area, bundle junction and appendages. The pressure drop is predicted in the fuel string region to be about 195 kPa at the low power and 317 kPa at the high power. At the low power, the pressure distribution is relatively linear over the fuel string corresponding to the single-phase pressure-loss characteristic. Boiling has not been initiated due to the low fuel-string power. However, at the high power, the pressure distribution is non-linear over the fuel string corresponding to the two-phase pressure loss characteristics. Boiling has been initiated at the upstream bundle due to high power. A total of about 44 kPa in pressure loss is predicted in the outlet branch region at the low power. At the high power, the pressure drop increases from 44 kPa to 56 kPa due to boiling. The majority of this pressure loss is due to the gravity effect over the 4-m length from the top of the fuel string to the outlet branch (see Figure 1).

3.2. Pressure Profiles in the U-2 Loop

The outlet pressure and mass flow rate in the U-2 loop have been maintained at about 10.16 MPa and 20 kg.s^{-1}, respectively, with a range of inlet-fluid temperatures meeting requirements of either experiments or Critical Power Ratios (CPR). As an illustration, two fuel strings are assembled for insertion into Channel E-20 and Channel O-17 of the loop. The fuel string for Channel E-20 (the inlet end) consists of three CANFLEX bundles, two 37-element bundles, and a material-test bundle, and the one for Channel O-17 has two CANFLEX bundles and four 37-element bundles. The nominal pressure (i.e., 10.16 Mpa) and mass flow rate (i.e., 20 kg.s^{-1}) are adopted with an inlet-fluid temperature of 262°C in this calculation. Pressure drops are calculated at two powers (total of these two strings): one at 5265 kW and the other at 7640 kW.

The pressure-drop model is applied to establish axial pressure profiles along the U-2 loop for the two powers. Figure 3 illustrates the calculated axial pressure profiles. The pressure loss over the fuel string is generally larger than that over the inlet-flow, connecting-pipe, and outlet-flow regions. Table 2 lists the calculated pressure drop at each region of the U-2 loop. The overall pressure loss is predicted to be 552 kPa at the low power and 694 kPa at the high power in the loop.

Table 2 Pressure Drops over Various Regions of the U-2 Loop

	Pressure Drop (kPa)					
	Inlet	Upstream String	Connecting Pipe	Downstream String	Outlet	Overall
Power = 5265 kW	-2	232	14	263	45	552
Power = 7640 kW	-2	239	16	384	57	694

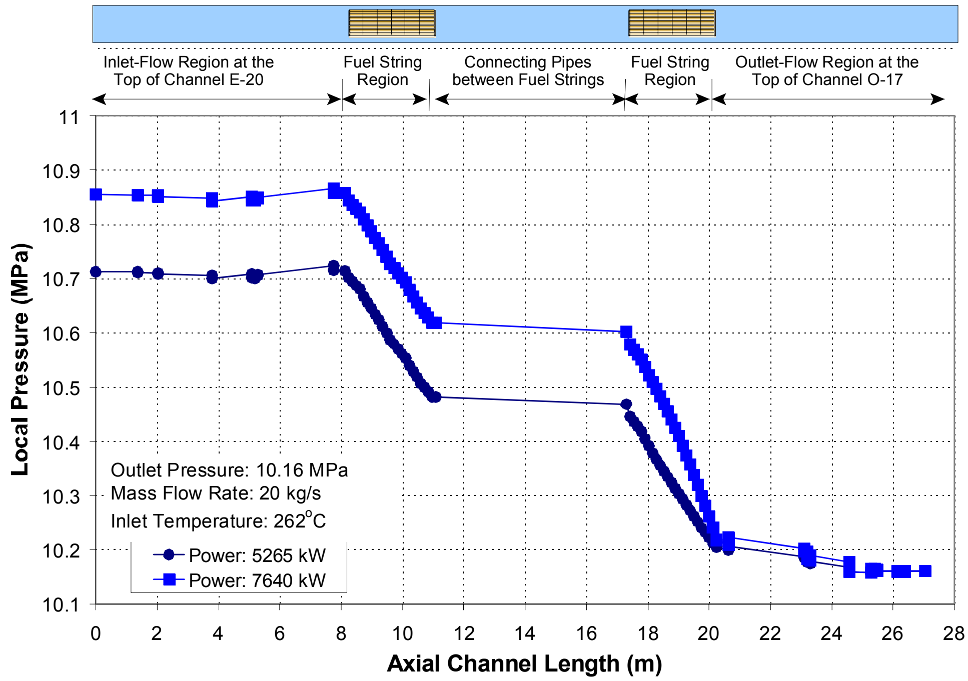

Figure 3 Pressure Profiles along the U-2 Loop

The pressure drop is negligible at the inlet-flow region of the loop. This is attributed to the compensating effect between frictional and gravitational components for the downward flow over this section. A sharp pressure drop is predicted over the fuel-string region, and corresponds to about half of the overall pressure drop. The pressure drop over the connecting-pipe region is smaller than that over the fuel string region (detailed variation over components in this region is not shown). Pressure drops between the upstream and downstream fuel strings are comparable due to similar hydraulic characteristics for CANFLEX and 37-element bundles at constant mass flow rate. The pressure drop over the upstream outlet-flow region is higher than that over the downstream outlet-flow region, due mainly to the gravity effect.

The pressure drop increases considerably at the high power due to the initiation of boiling at locations close to the downstream end of the upstream string. This has led to a slight increase in pressure drop over the upstream string (i.e., 232 kPa at the power of 7640 kW as compared to 239 kPa at the power of 5265 kW). The two-phase mixture travels over the connecting-pipe region with a further increase in pressure drop. Overall, the increase is small over these two regions since the flow quality remains low. A sharp increase in pressure drop is predicted over the downstream fuel string at the power of 7640 kW (384 kPa as compared to 263 kPa at the power of 5265 kW corresponding to about a 50% increase), and is attributed to the bulk-boiling effect. This effect remains significant at the outlet-flow region.

4. CONCLUSIONS AND FINAL REMARKS

- A pressure-drop model has been developed for the U-1 and U-2 loops of the NRU reactor. It provides local pressure distributions between instrument locations at inlet-flow and outlet-flow regions.
- Piping components and fuel-string assemblies are modeled separately for single-phase and two-phase flows. The overall pressure loss comprises frictional and form losses, and changes due to acceleration and gravity. Relevant models have been introduced to the calculation for these pressure drops in single-phase flow. The single-phase pressure losses are multiplied by the homogeneous two-phase multiplier or a modified form of the homogenous two-phase multiplier to provide two-phase pressure losses.
- Detailed pressure profiles have been established along the U-1 and U-2 loops at two typical powers. The pressure loss over the fuel string is generally larger than that over the inlet, connecting, and outlet piping components. A linear pressure profile has been observed over the fuel string at low power, indicating single-phase flow in the channel. The pressure profile becomes non-linear at high power, signifying the presence of two-phase flow at the downstream end. Different combinations of fuel type in the string appear to have little impact on the pressure profile. This is mainly due to the similarity of pressure-drop characteristics of the fuel types used in fuel irradiation experiments.
- A few simplifying assumptions have been introduced to facilitate the analysis (e.g., the pressure-drop characteristic of the upper-flux suppressor). These assumptions should be reviewed in the future to improve the prediction accuracy. Pressure-loss experiments may be needed for specific components to reduce the prediction uncertainty, if needed.

5. ACKNOWLEDGEMENT

The authors gratefully acknowledge the contributions of Erin Sullivan, William Simmons, Ian Lusk, and Joe Martin.

6. NOMENCLATURE

a	constant in Equation 17
b	constant in Equation 17
C	percentage of diametral creep
D	diameter, m
$D_{P/T}$	pressure-tube diameter, m
D_{ref}	inside diameter of the flow tube of the reference full-scale bundle tests, m
f	friction factor
g	gravitational acceleration (= 9.806 $m \cdot s^{-2}$)
G	mass flux, $kg/m^2 \cdot s$

K	loss coefficient
L	length of the channel, m
ΔP	pressure drop, kPa
x	vapour-mass quality
x_a	vapour-weight quality in the bundle
x_{th}	thermodynamic quality
Δz	change in elevation, m

Greek Letters

α	void fraction
ε	roughness height, m
ϕ^2	two-phase multiplier
μ	dynamic viscosity, kg/m·s
ν	specific volume, m^3/kg
ρ	density, kg/m^3

Subscripts

a	acceleration
app	appendages; mid plane spacer and buttons
b	bulk-liquid
bp	bearing-pad plane
but	button plane
cc	channel creep
cont	contraction
cor	correction
CW	Colebrook-White
exp	expansion
f	friction
form	form losses
fuel	fuel bundle
g	gravity
j	junction or junction plane
hy	hydraulic
k	form-loss

l	liquid
LO	liquid (assuming the total flow to be liquid)
mpm	most-probable misaligned
OFS	outside the fuel string
P/T	pressure-tube
ref	reference full-scale bundle tests
s	middle plane with spacers and bearing pads
sp	single-phase
th	thermodynamic
tp	two-phase
uncrept	uncrept channel
v	vapour

Dimensionless Groups

Re	Reynolds number

Abbreviations

AECL	Atomic Energy of Canada Limited
CANDU	CANada Deuterium Uranium (nuclear reactor)
CANFLEX	CANDU Flexible
NRU	National Research Universal

7. REFERENCES

1. Wallace, D.J. and Hartmann, W., "A Review of NUCIRC Development in Support of CANDU Plant Aging Assessments", Proc. 6th Int. Conf. on Simulation Methods in Nuclear Engineering. Montréal, Québec, Canada. Oct. 12-15, 2004.
2. Chen, N.H., "An Explicit Equation for Friction Factor in Pipe", Industrial and Engineering Chemistry: Fundamentals, Vol. 18, 1979, pp. 296-297.
3. Idelchik, I.E., "Handbook of Hydraulic Resistance", Hemisphere Publishing Corporation, 1986.
4. Massena, W.A., "Steam-Water Pressure Drop and Critical Discharged Flow – A Digital Computer Program", General Electric, Hanford Atomic Products Operation Report, HW-65706, 1960.